Fabrication of PECVD-grown fluorinated hydrocarbon nanoparticles and circular nanoring arrays using nanosphere lithography

D.K. Sarkar,

M. Farzaneh

Industrial Chair on Atmospheric Icing of Power Network Equipment (CIGELE) and Canada Research Chair on Atmospheric Icing Engineering of Power Networks (INGIVRE) at Université du Québec à Chicoutimi, Québec, Canada

Abstract

Nanosphere lithography (NSL) masks were created by spin-coating of polystyrene particles onto silicon surfaces. Fluorinated hydrocarbon films were coated on the nanosphere lithography masks using plasma-enhanced chemical vapor deposition (PECVD) to obtain ordered arrays of fluorinated hydrocarbon. Atomic force microscope images show hexagonally ordered nanodots of dimension 225 ± 11 nm with a height of 23 ± 4 nm. Every hexagon encloses a circular ring of diameter 540 ± 24 nm having a height and width of 13.5 ± 0.6 nm and 203 ± 16 nm, respectively. FTIR analysis shows two distinct zones of atomic bonding of CH_x and CF_x in the plasma coated ordered fluorinated hydrocarbon films.

1. Introduction

Nanometer size dielectric, semiconductor, and metallic structures have received a great deal of attention lately due to their interesting physical properties and vast range of

potential applications [1], [2], [3], [4] and [5]. For example, nanometric coatings can be used as optical devices [1], electronic devices to create large flat screen display [2], the dielectric coatings can be used as gate oxide for CMOS devices [4] and metal nanoparticles incorporated dielectric films can be used in electrical switching devices [5]. Recently, Sarkar et al. have intensively investigated structural, chemical, optical, electrical as well as surface morphological properties of several nanostructured thin films [4], [5], [6] and [7].

Photolithography and electron beam lithography techniques are routinely used to prepare ordered micro/nanostructures [8]. The alternative to these techniques are the relatively inexpensive nanoimprint [9] and nanosphere lithography (NSL) [10], [11] and [12]. Nanosphere lithography has been used recently for its simplicity in creating well-ordered metallic nanodots by electron beam evaporation [10], ordered semiconductor patterns by reactive ion etching [11], and ordered metal oxides by drop coating process [12]. Nevertheless, the plasma-enhanced chemical vapor deposition (PECVD) technique has not been used yet to prepare ordered nanopatterns utilizing the NSL mask, having the potential to be used in different technological applications [13], [14] and [15].

In this paper, we report the design of fluorinated hydrocarbon, as a representative of plasma coating, nanoparticle arrays using nanosphere lithography. The masks of nanosphere lithography patterns were created by spin-coating 1-µm polystyrene spheres followed by fluorinated hydrocarbon coating using PECVD and by the removal of polystyrene microspheres. The creation of hexagonally-ordered nanodots of size 225 ± 11 nm with a height of 23 ± 4 nm and circular ring of diameter 540 ± 24 nm has been achieved in this work.

2. Experimental

The subsequent steps involved in creating nanopatterned fluorinated hydrocarbon were (i) spin-coating of micrometer-sized spherical polystyrene particles, (ii) PECVD coating of fluorinated hydrocarbon, and (iii) chemical etching of polystyrene microspheres. Silicon surfaces were spin coated (spin coater, Laurell Technologies corporation) using a polystyrene bead solution prepared by mixing 350 µl of polystyrene microsphere beads of diameter 1 µm (Cat#07310-15, Polysciences Inc.) in 50 µl of Triton X-100 (Sigma–Aldrich) diluted with methanol by 1:400 in volume ratio [11]. The spin-coating process of the polystyrene bead solution consists of three consequent steps: (i) 400 rpm for 10 s to

spread the bead solution evenly; (ii) 800 rpm for 2 min to spin away the excess bead solution; (iii) 1400 rpm for 10 s to spin off the excess materials from the edges. Fluorinated hydrocarbon coatings were carried out using inductively coupled PECVD by applying a power of 100 W in the RF-source in presence of three gases (Ar, CH4, C2F6) with a flow ratio of 40:14:7 (in sccm) maintaining a total pressure of 20 mTorr in a high-vacuum chamber (base pressure ~2 × 10–6 Torr). A bias voltage of –50 V was applied to the substrate holder while coating. The fluorinated hydrocarbon-coated nanosphere lithography mask was immersed in cyclohexane and placed in an ultrasound bath for 20 min to remove polystyrene microparticles. The microstructure of these films was investigated using field emission scanning electron microscopy (FESEM, LEO 1525) and an atomic force microscope (AFM) (Digital Nanoscope IIIa by Digital Instruments). Atomic bonding of the fluorinated hydrocarbon was characterized using Fourier transform infrared spectroscopy (FTIR) (Perkin-Elmer Spectrum One).

3. Results and discussions

Fig. 1(a) and (b) shows AFM and SEM images, respectively, of the nanosphere lithography mask of polystyrene microsphere on silicon surfaces. These images show that the polystyrene microspheres are hexagonally packed in two dimensions producing a nearly triangular aperture formation between any three spheres. The area of this triangular aperture is related to the radius of the sphere by the following equation:

Equation (1)

$$A_\Delta = \left(\sqrt{3} - \frac{\pi}{2} \right) R^2$$

where $A\Delta$ is the area of the triangular aperture and R is the radius of the sphere. If an equilateral triangle would be formed using this area given by Eq. (1), the side of the triangle would be found by the following equation:

Equation (2)

$$a_\Delta = \left(4 - \frac{2}{\sqrt{3}} \pi \right)^{1/2} R = 0.61R$$
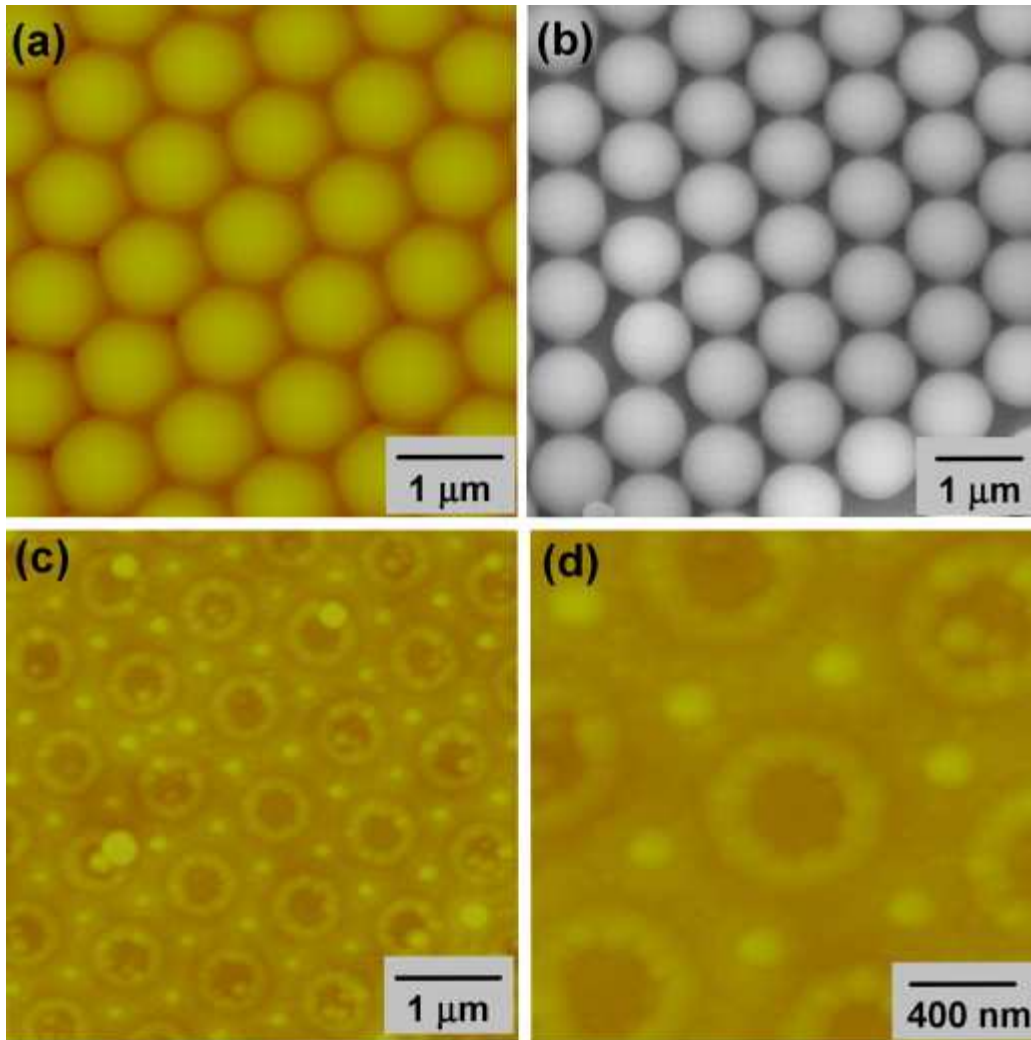
where $a\Delta$ is the side of the triangle.

Fig. 1.
(a) AFM image of nanosphere lithography (SPL) mask, (b) SEM image of nanosphere lithography (NPL) mask, (c) AFM image of hexagonally pattern nanodots and microrings of fluorinated hydrocarbon, (d) zoomed view of (c).

From Eq. (2) it can be seen that a triangular nanodot of side 305 nm can be formed when the radius of the microsphere is 500 nm (diameter 1 µm). Fig. 1(c) shows the AFM image of uniform, hexagonally patterned nanodots of fluorinated hydrocarbon. These dots resemble more like spheres rather than expected triangles as usually observed in the physical vapor deposition (PVD) processes [10] and [16]. AFM analyses show that the size of the nanodots is 225 ± 11 nm with a height of 23 ± 4 nm. These nanodots are separated by 585 ± 14 nm on the contour of a hexagon and diametrically 1.20 ± 0.04 µm apart. The calculated value of the separation between the dots is 577 nm with a

diametrically opposite distance of 1.15 μm for 1 μm diameter PS particles in the NSL mask. The sizes of the observed nanodots are smaller than the expected triangle as predicted by Eq. (2). However, their separation on the hexagonal contour, as observed by AFM, is very close to the calculated value. The reduced size of the fluorinated hydrocarbon nanodots as compared to the calculated value could be due to the continuous ion bombardment during plasma deposition process. The ion bombardment increases the mobility of the different fragments of the coating materials on the surface resulting in compact dots. This process may be comparable to the thermal annealing process employed by Tan et al. [10] in which the triangular dots of gold turns into nearly spherical dots with reduced size due to surface mobility of gold at elevated temperatures. The size of the as-grown triangular gold nanodots of 287 nm, as observed by those authors, reduced to 226 and 190 nm following annealing at 325 and 930 °C, respectively [10]. According to Eq. (2), the expected as-grown size of the triangular gold dot would be 321 nm in their study as the size of the polystyrene microsphere used was 1053 nm [10]. Usually, reported sizes of the as-grown triangular nanodots are smaller than that predicted by Eq. (2) as observed by us and reported in the literatures [10] and [16].

It is also observed in our study that every hexagon formed by the nanodots encloses a circular ring. Fig. 1(d) shows an AFM image of ordered fluorinated hydrocarbon rings (magnified presentation of Fig. 1(c)). The diameter of these rings is found to be 540 ± 24 nm with their centers separated by 1 μm. The height and width of the rings are 13.5 ± 0.6 and 203 ± 16 nm, respectively. In the PECVD process, the deposited fragments have higher mobility on the surface due to the collisions between them and their higher energy, as compared to the PVD process. Therefore, the materials tend to move under the spheres and get deposited as a ring around it. However, in the case of PVD process (e-beam or thermal evaporation) the deposition is more of line-of-sight deposition. Therefore, no or little under-deposition would be expected. Hence, to our knowledge, no reports in the literature are found on the formation of ring in the PVD process while using NSL mask [10] and [16]. However, ring formations were reported in the chemical process possibly due to the easy motion of the liquid under the NSL masks [12] and [17]. Though, in our study, the surfaces are mostly covered by the spherical nanodots and circular rings, a few scattered triangular nanodots are also found as observed in PVD processes [10] and [16]. The 2D ordered nanostructured arrays produced by NSL mask using PVD process have extensive applications in surface

plasmon sensor arrays [18], nanometre-sized magnetic domains with orientation dependent magnetic anisotropy [19] and cobalt silicide nanodots on Si(0 0 1) substrates for the applications of semiconductor devices [20]. To the best of our knowledge, no reports have been found in the literature on the fabrication or applications of ordered hydrocarbon or fluorinated hydrocarbon nanodots formation using PECVD utilizing NSL mask. However, PECVD grown ordered hydrocarbon or fluorinated hydrocarbon nanostructured films produced though NSL mask might have great potential in several areas such as in superhydrophobic coatings [21] and [22], antibacterial applications [23], interlayer dielectrics because of its low dielectric constant [24], nanocrystalline diamond resonator array for the application of RF signal processing [25], etc.

Fig. 2 shows the FTIR spectrum of the nanodots consisting of fluorinated hydrocarbon. The two distinct zones of CFx and CHx bands are located in the range of 800–2000 and 2700–3200 cm−1, respectively. Though the main CFx peaks are situated in the 800–2000 cm−1 range, some of their bond characteristics are as thus: (i) A broad band in the region of 950–1400 cm−1 is associated with the CF, CF2 and CF3 stretching modes [26]. The strong absorption peak at approximately 1170 cm−1 is due to CF2 symmetric stretching bonds. The position of this peak was previously reported to be at 1153 cm−1[27] and 1180 cm−1[28]. A shoulder appearing at approximately 1265 cm−1 is due to the asymmetric vibration of the CF2 peak which was reported to be at 1253 cm−1[26]. (ii) The broad band centered at 1660 cm−1 is due to a C$=$C stretching mode associated with the presence of HFC$=$C< fragments in the fluorinated hydrocarbon films [27] and [29]. Finally, the band in the range of 2800–3100 cm−1 is assigned to the CHx bonds. The two peaks at 2870 and 2945 cm−1 correspond to sp3–CH2 symmetric vibrational frequencies and sp3–CH2 asymmetric vibrational frequencies, respectively [30], and were reported to be at 2850 and 2920 cm−1[30]. The bands in the two zones (800–2000 cm−1 and 2700–3200 cm−1) of the FTIR spectrum confirm the presence of fluorinated hydrocarbon formation by the PECVD process.
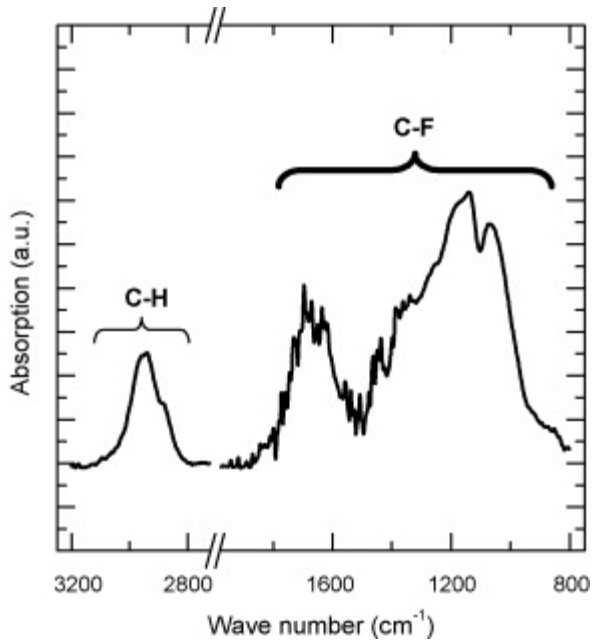
Fig. 2.
FTIR spectrum of the nanostructured fluorinated hydrocarbon.

4. Conclusions

Polystyrene particles were spin-coated on silicon surfaces to produce nanosphere lithography masks. Plasma-enhanced chemical vapor deposition was used to coat fluorinated hydrocarbon films on the lithographic mask. Hexagonally-ordered patterns of fluorinated hydrocarbon nanodots were observed after the removal of polystyrene particles. The sizes of the nanodots are 225 ± 11 nm and are separated by 585 ± 14 nm forming a hexagonal pattern, each hexagon enclosing a nanoring of diameter 540 ± 24 nm. The characteristic bands of the C—F and C—H bonds observed by FTIR confirm that the nanodots are composed of fluorinated hydrocarbon.

Adomou for the fabrication of 2D polystyrene particles on silicon surfaces by spin-coating method.

References

[1] C.J. Kiely, J. Fink, M. Brust, D. Bethell, D.J. Schiffrin
Nature, 396 (1998), p. 444
[2] R.F. Service
Science, 278 (1997), p. 383
[3] M.J. Yacaman, J.A. Ascencio, H.B. Liu, J.G. Torresdey
J. Vac. Sci. Technol. B, 19 (2001), p. 1091
[4] D.K. Sarkar, D. Brassard, M.A. El Khakani
Appl. Phys. Lett., 87 (2005), p. 253180
[5] D.K. Sarkar, F. Cloutier, M.A. El Khakani
J. Appl. Phys., 97 (2005), p. 084302
[6] D.K. Sarkar, D. Brassard, M.A. El Khakani, L. Ouellet
Thin Solid Films, 515 (2007), p. 4788
[7] D.K. Sarkar, E. Desbiens, M.A. El Khakani
Appl. Phys. Lett., 80 (2002), p. 294
[8] S.Y. Chou, M.S. Wei, P.R. Krauss, P.B. Fischer
J. Appl. Phys., 76 (1994), p. 6673
[9] S.Y. Chou, P.R. Krauss, P.J. Renstrom
Science, 272 (1996), p. 85
[10] B.J.Y. Tan, C.H. Sow, T.S. Koh, K.C. Chin, A.T.S. Wee, C.K. Ong
J. Phys. Chem. B, 109 (2005), p. 11100
[11] C.L. Cheung, R.J. Nikolić, C.E. Reinhardt, T.F. Wang
Nanotechnology, 17 (2006), p. 1339
[12] Y. Li, W. Cai, G. Duan, B. Cao, F. Sun, F. Lu
J. Colloid Interf. Sci., 287 (2005), p. 634
[13] R. d'Agostino, R. Lamendola, P. Favia, A. Giquel
J. Vac. Sci. Technol. A, 12 (1994), p. 308
[14] D. Levchuk
Surf. Coat. Technol., 201 (2007), p. 6071
[15] X. Liu, R.K.Y. Fu, C. Ding, P.K. Chu

Biomol. Eng., 24 (2007), p. 113

[16] J.C. Hulteen, D.A. Treichel, M.T. Smith, M.L. Duval, T.R. Jensen, R.P. Van Duyne

J. Phys. Chem. B, 103 (1999), p. 3854

[17] Y. Li, W. Cai, B. Cao, G. Duan, F. Sun

Polymer, 46 (2005), p. 12033

[18] A.D. Ormonde, E.C. Hicks, J. Castillo, R.P. Van Duyne

Langmuir, 20 (2004), p. 6927

[19] M. Albrecht, G. Hu, I.L. Guhr, T.C. Ulbrich, J. Boneberg, P. Leiderer, G. Schatz

Nat. Mater., 4 (2005), p. 203

[20] S.L. Cheng, S.W. Lu, S.L. Wong, C.C. Chang, H. Chen

J. Cryst. Growth, 300 (2007), p. 473

[21] D.K. Sarkar, M. Farzaneh, R.W. Paynter, Mater. Lett., in press.

[22] A. Safaee, D.K. Sarkar, M. Farzaneh, Appl. Surf. Sci., in press.

[23] M. Ishihara, T. Kosaka, T. Nakamura, K. Tsugawa, M. Hasegawa, F. Kokai, Y. Koga

Diamond Relat. Mater., 15 (2006), p. 1011

[24] K. Endo, K. Shinoda, T. Tatsumi

J. Appl. Phys., 86 (1999), p. 2739

[25] J.W. Baldwin, M.K. Zalalutdinov, T. Feygelson, B.B. Pate, J.E. Butler, B.H. Houston

Diamond Relat. Mater., 15 (2006), p. 2061

[26] C.E. Bottani, A. Lamperti, L. Nobili, P.M. Ossi

Thin Solid Films, 433 (2003), p. 149

[27] A.C. Rastogi, S.B. Desu

Appl. Phys. A, 83 (2006), p. 57

[28] P. Favia, G. Cicala, A. Milella, F. Palumbo, P. Rossini, R. d'Agostino

Surf. Coat. Technol., 169–170 (2003), p. 609

[29] H. Ykomichi, A. Masuda

J. Appl. Phys., 86 (1999), p. 2468

[30] X. Yan, T. Xu, G. Chen, S. Yang, H. Liu

Appl. Surf. Sci., 236 (2004), p. 328